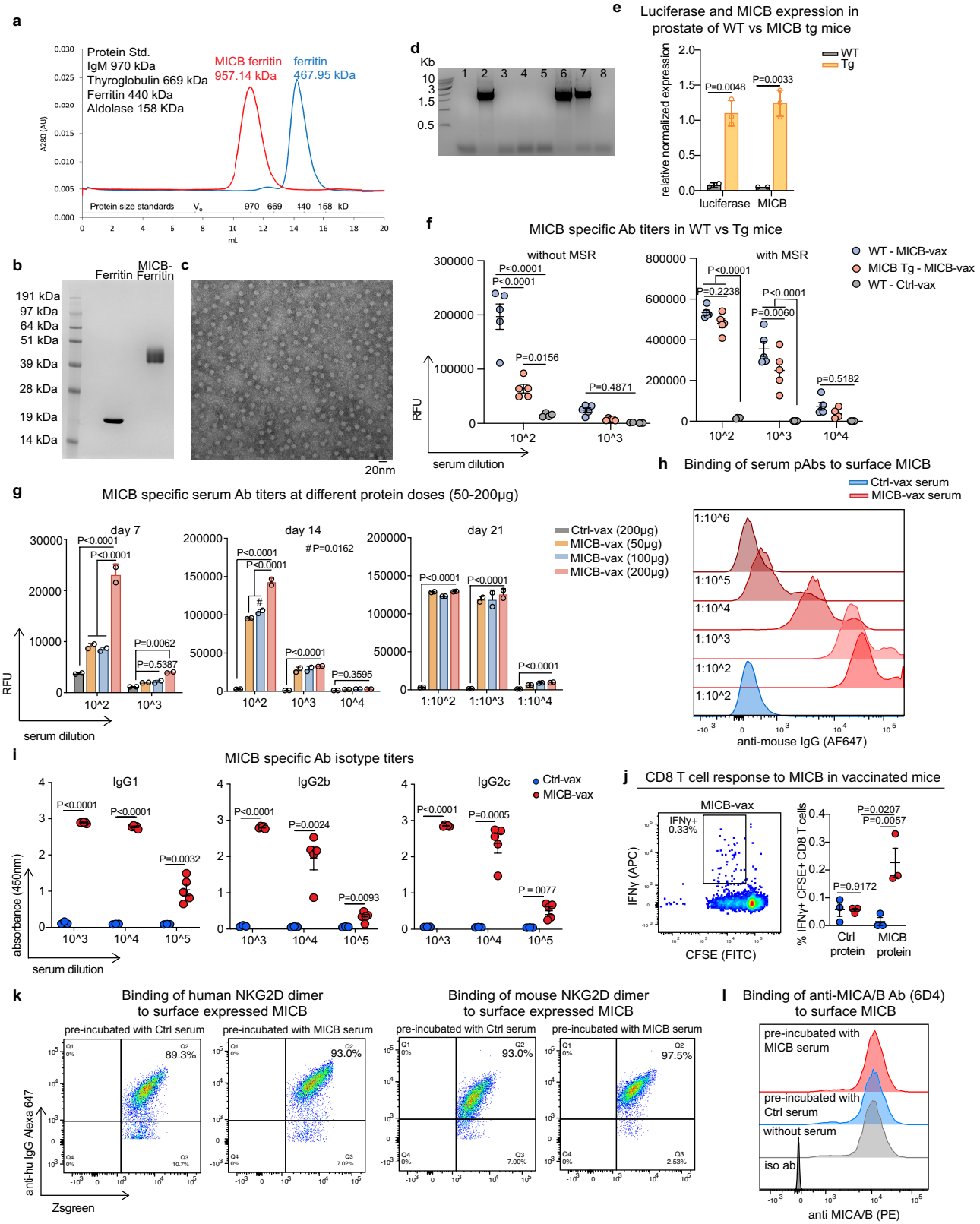

Extended Data Fig. 1 | See next page for caption.

Extended Data Fig. 1 | Characterization of vaccine targeting MICA/B vaccine α3 domain. a, HPLC gel filtration analysis of affinity-purified ferritin (immunogen for Ctrl-vax) and MICB-ferritin (immunogen for MICB-vax) proteins. The proteins formed nanoparticles of ~957 kDa (MICB-ferritin) and ~468 kDa (ferritin); molecular weight standards are indicated. **b**, SDS-PAGE analysis of purified ferritin and MICB-ferritin proteins under reducing conditions. **c**, Electron microscopy image showing MICB-ferritin protein assembled into nanoparticles (98,000x magnification). **d**, Identification of MICB transgenic (Tg) mice by PCR amplification using genomic DNA extracted from tail biopsies (lanes 2,6, MICB Tg; lane 7, positive control amplification from plasmid with the transgene cassette; lane 8, negative control reaction). **e**, Quantitative RT-PCR analysis of luciferase and MICB mRNA in the prostate of WT (grey) and MICB-tg (orange) mice (n = 2 WT, n = 3 MICB-Tg mice) normalized to mouse *Hprt* mRNA. **f**, Quantification of day 14 MICB-specific serum Ab titers (fluorescence-based immunoassay, DELFIA) in WT and MICB-tg mice immunized with Ctrl-vax (n = 4 mice/group) (grey) (120μg ferritin protein, 100μg CpG, 1μg GM-CSF) or MICB-vax (n = 5 mice/group) (200μg MICB-ferritin, 100μg CpG, 1μg GM-CSF) without MSR (left) or with MSR (right) scaffold. **g**, Quantification of MICB-specific serum Ab titers (fluorescence-based immunoassay, DELFIA) in mice immunized with Ctrl-vax (grey) or MICB-vax using differing protein doses, 50μg (yellow), 100μg (blue) or 200μg (red) (n = 2 mice/group). **h**, Representative flow cytometry plots showing binding of polyclonal serum Abs from mice immunized with Ctrl-vax (blue) or MICB-vax (red) to cell surface MICB on B16F10 (MICB) tumor cells; serum dilutions are indicated for each condition. **i**, Titers of MICB Ab isotypes assessed by ELISA (n = 5 mice/group) in MICB transgenic mice immunized with Ctrl-vax (blue) or MICB-vax (red). **j**, Analysis of MICB-specific CD8 T-cell responses in the spleen of mice immunized with Ctrl-vax (blue) or MICB-vax (red). Intracellular cytokine staining (IFNγ) and CFSE dilution is shown in representative flow cytometry plots (left); data are quantified for T-cells from both vaccine groups (3 mice/group, right). **k**, Analysis of human NKG2D dimer (left) and mouse NKG2D dimer (right) binding to cell surface MICB on B16F10 (MICB-ZsGreen) tumor cells pre-incubated with sera (5μl) from Ctrl-vax or MICB-vax mice. **l**, Representative flow cytometry plots showing binding of anti-human MICA/B antibody (6D4, specific for MICA/B α1-α2 domains) to cell surface MICB on B16F10 (MICB) tumor cells pre-incubated with sera from mice immunized with Ctrl-vax (blue) or MICB-vax (red). Representative data from >3 independent experiments (**a**, **b**). Data from a single experiment with technical replicates (**c**). Representative data from three experiments (**d, e, g, h, i**). Representative data from two experiments (**j, k, l**). Two-tailed unpaired Student's t-test **(e);** Two-way ANOVA with Tukey's multiple comparison test (**f, g**); Two-way ANOVA with Sidak's multiple comparison test (**i, j**). Data depict mean +/− SD (**e**,**g**) or mean +/− SEM (**f, i, j**).

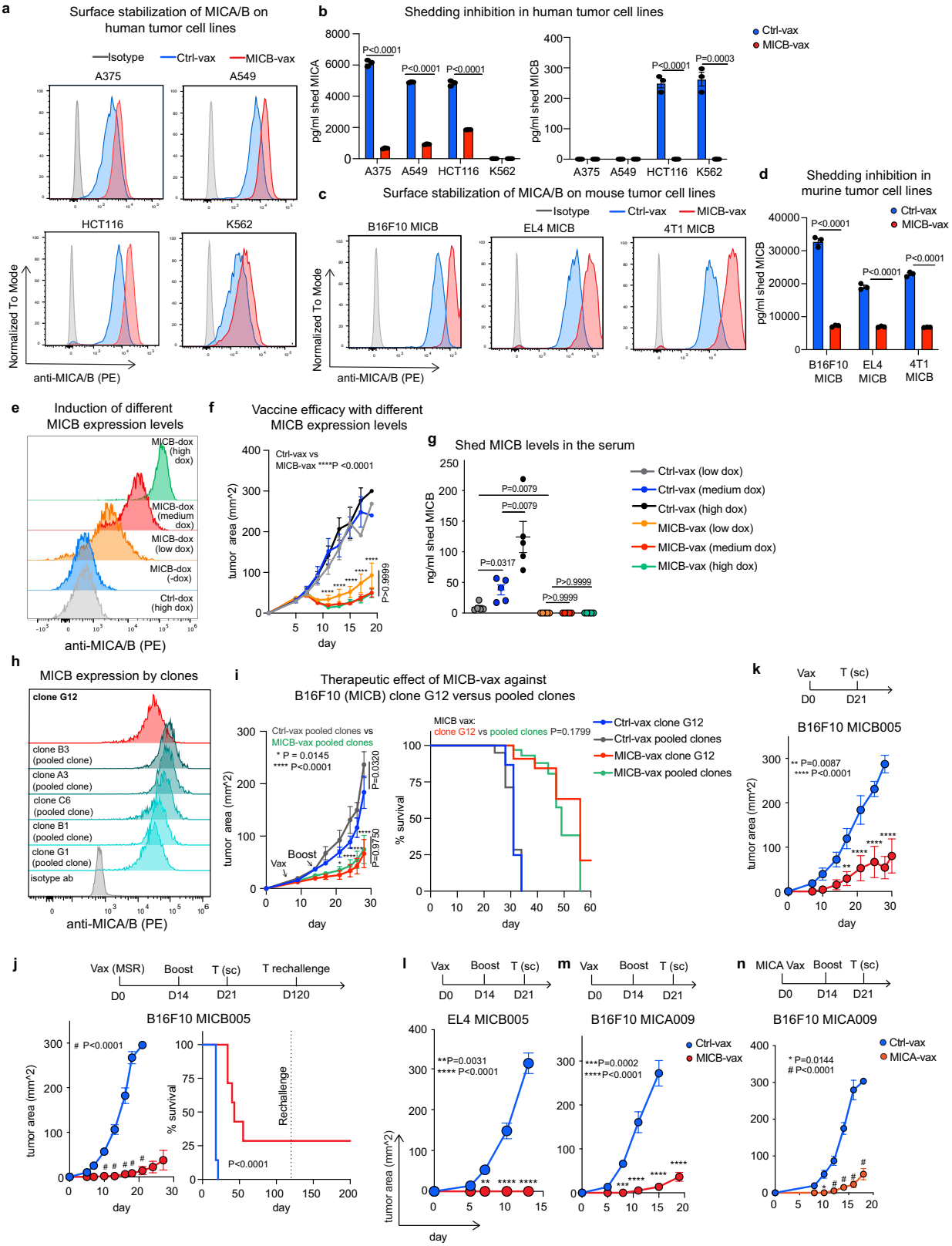

Extended Data Fig. 2 | See next page for caption.

Extended Data Fig. 2 | Characterization of vaccine-induced immune responses. a, b, Inhibition of MICA/B shedding and surface stabilization by vaccine-induced Abs. Flow cytometric analysis of cell surface MICA/B levels (**a**) and shed MICA/B in supernatants (**b**) for human A375 melanoma, A549 lung carcinoma, HCT116 colon carcinoma and K562 myelogenous leukemia cell lines 24 h following incubation with 10 µl of sera from Ctrl-vax (blue) or MICB-vax (red) immunized mice; isotype control Ab staining shown in grey (**a**). **c**, **d**, Inhibition of MICB shedding and surface stabilization by vaccine-induced Abs on mouse tumor cell lines. Flow cytometric analysis of cell surface MICB levels (**c**) and shed MICB in supernatants (**d**) for mouse B16F10 (MICB) melanoma, EL4 (MICB) lymphoma and 4T1 (MICB) triple negative breast cancer cell lines 24 h following incubation with 10 µl of sera from Ctrl-vax (blue) or MICB-vax (red) immunized mice. Isotype control Ab staining shown in grey (**c**). **e**–**g**. Vaccine efficacy at different MICB expression levels induced in tumor cells using a doxycycline (dox) inducible promoter. Representative flow cytometry histograms showing MICB surface expression levels on B16F10 (MICB-dox) tumors *in vivo* in mice treated with PBS (blue histogram) or different concentrations of doxycycline (dox): low dox (2.5mg/kg, orange), medium dox (5mg/kg, red) or high dox (10mg/kg, green) or control B16F10 (Ctrl-dox) tumors treated with high dox (10mg/kg, grey) (**e**). Analysis of B16F10 (MICB-dox) tumor growth kinetics at different MICB expression levels by tumor cells. Mice received Ctrl-vax (grey, blue, black) or MICB-vax (orange, red, green) on day 0 and a boost on day 14. B16F10 (MICB-dox) tumor cells were implanted on day 21, and MICB expression was induced on tumor cells on day 25 when tumors were palpable by treating mice with different concentrations of doxycycline as indicated (**f**) (n=7 mice/group). Quantification of serum levels of shed MICB in mice immunized with Ctrl-vax (grey, blue, black) or MICB-vax (orange, red, green) 96 h post dox-mediated induction of MICB on B16F10 (MICB-dox) tumor cells. Serum levels of shed MICB were analyzed in 5 randomly selected mice in each group (**g**). **h**–**i**, Representative flow cytometry histogram showing surface MICB levels on B16F10 (MICB) clone G12 (red) or indicated pooled clones (gradient of turquoise). Grey histogram represents isotype antibody staining of B16F10 (MICB) clone G12 (**h**). Assessment of therapeutic efficacy of MICB-vax (red, green) or Ctrl-vax (blue, grey) in mice with tumors established with B16F10 (MICB) clone G12 or pooled clones (B3, A3, C6, B1, G1) (n=8 mice/group) (**i**). **j**–**n**, Assessment of vaccine efficacy targeting MICA or MICB α3 domains. The MSR scaffold was formulated with antigens, GM-CSF and CpG. Mice received one or two doses of Ctrl-vax, MICB-vax (**j**–**m**) or MICA-vax (**n**) and were then challenged with B16F10 tumor cells expressing MICB (allele 005) (**j, k**) or MICA (allele 009) (**m, n**) or EL4 tumor cells expressing MICB (allele 005) (**l**). Vaccination and tumor challenge schedule is illustrated above each experiment; n = 7 mice/group (**j**–**l**), n = 6 mice in Ctrl-vax, n = 8 mice in MICB-vax (**m**) and n = 6 mice/group (**n**). For experiments shown in (**j**), tumor-free mice were rechallenged on day 120 using the same dose of B16F10 (MICB) tumor cells as in the initial inoculation. Representative data from two experiments (**a**–**d, j**–**n**). Data from single experiment (**e**–**g, h**–**i**). Two-tailed unpaired Student's t-test (**b, d**); one-way ANOVA with Tukey's multiple comparison test (**g**); two-way ANOVA with Bonferroni's post hoc test (**f, i** (left), **j** (left), **k. l, m, n**); log-rank (Mantel-Cox) test (**i** (right), **j** (right). Data depict mean +/− SD (**b, d**) or mean +/− SEM (**f, g, i**–**n**).

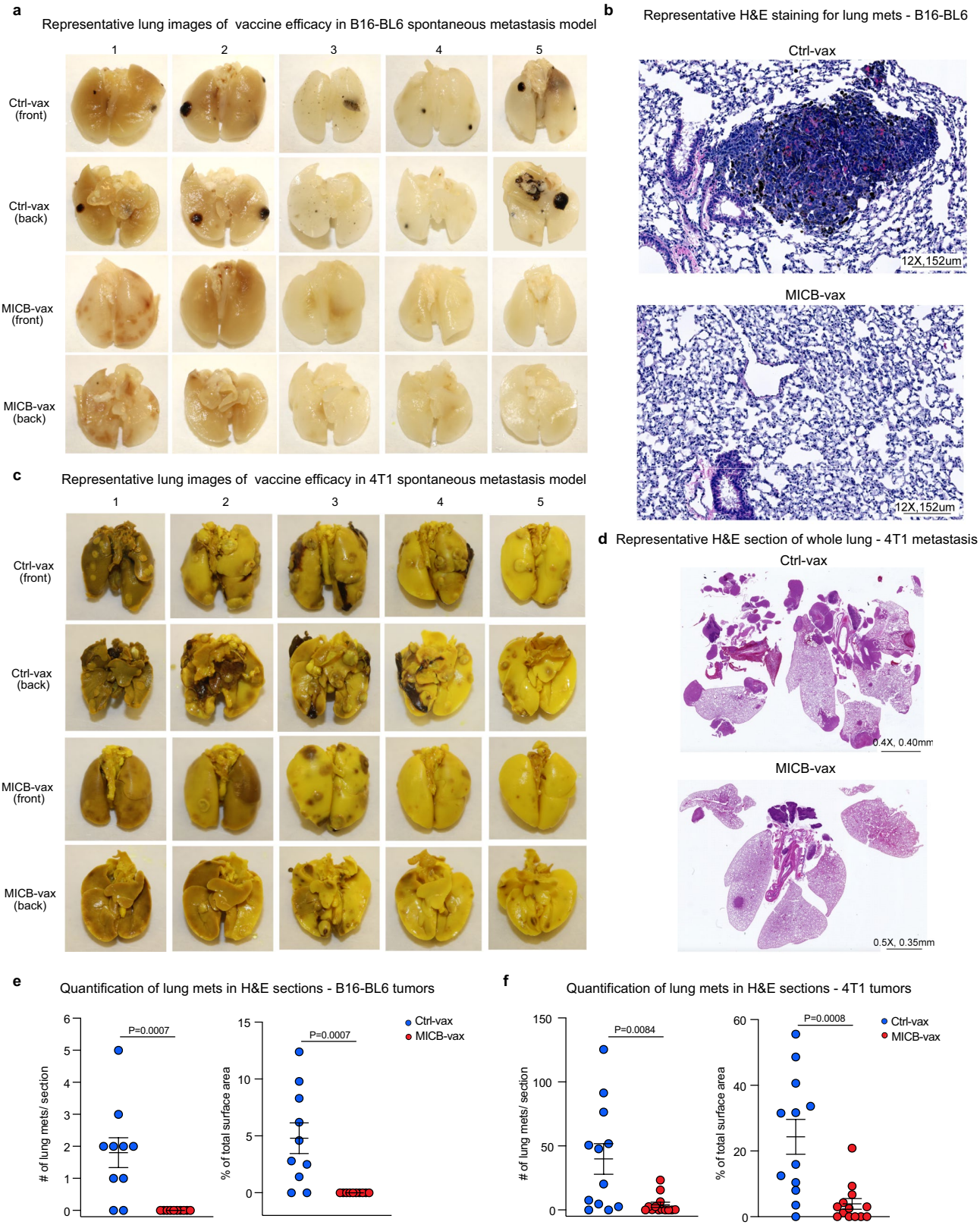

Extended Data Fig. 3 | Protection from metastatic disease by vaccination following surgical removal of primary tumors. a, **c**, Images of lung metastases from five representative mice per group immunized with Ctrl-vax (top two rows) or MICB-vax (bottom two rows). Mice were immunized following surgical removal of primary B16-BL6 (MICB) (n = 10 mice/group) (**a**) and 4T1 (MICB) (**c**) tumors (n = 13 mice/group), as described in Fig. 1f, g. **b**, **d**, Representative bright field images of H&E stained histological sections of lung metastases from mice with B16-BL6 (MICB) (**b**) or 4T1 (MICB) (**d**) tumors. **e**–**f**, Quantification of the number of metastases per H&E stained section (left) and percentage of area of lung section occupied by metastases (right) for mice immunized with Ctrl-vax (blue) or MICB-vax (red) following surgical removal of primary B16-BL6 (MICB) tumors (**e**) or 4T1 (MICB) tumors (**f**). Representative data from two experiments (a-f). Representative images of 5 histological lung sections per mouse (**b, d**), Two-tailed Mann Whitney test (**e**, **f**). Data depict mean+/− SEM.

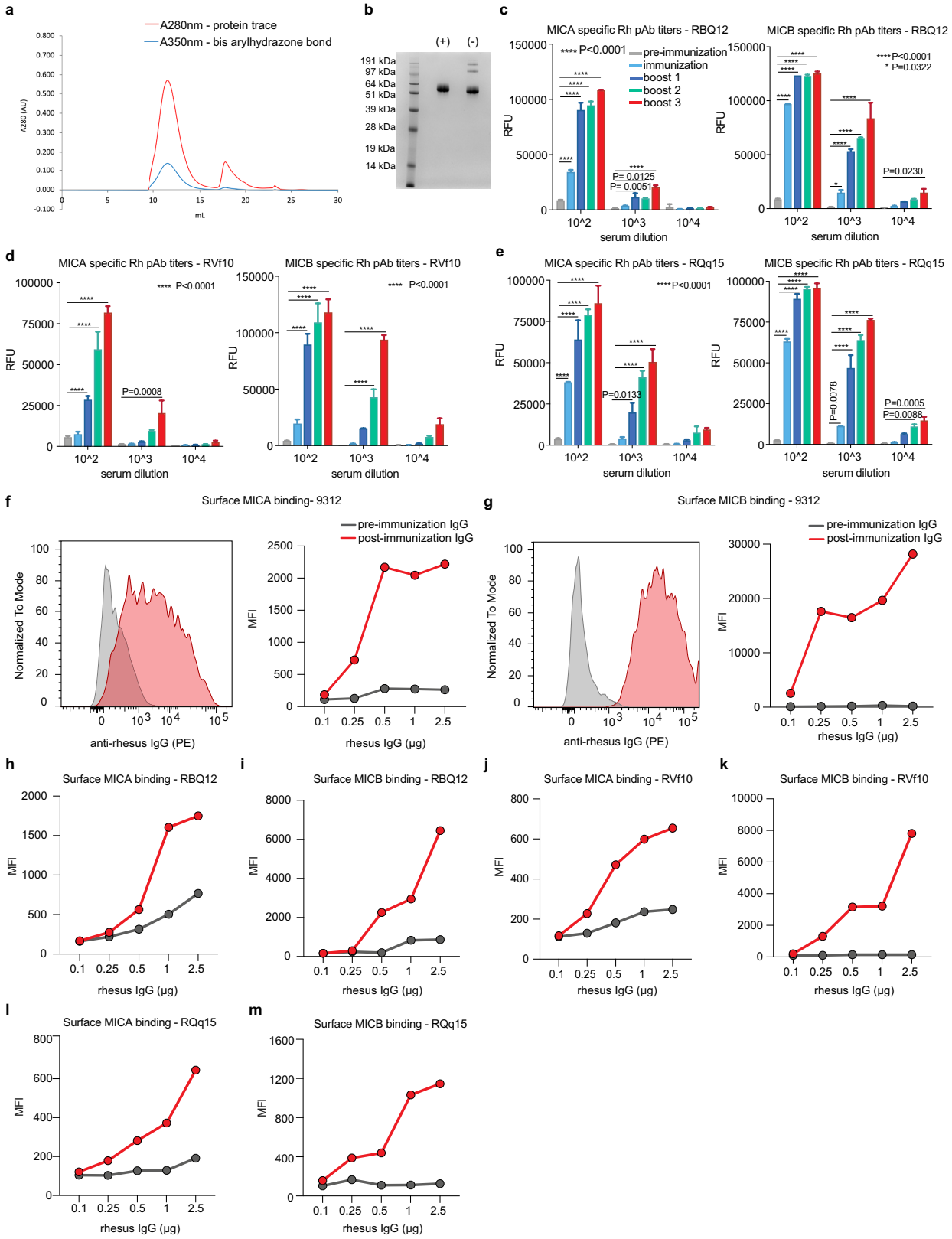

Extended Data Fig. 4 | See next page for caption.

Extended Data Fig. 4 | Immunogenicity of MICA/B α3 domain vaccine in non-human primates. a, Characterization of the MICA/B α3 immunogen used in the primate study. The α3 domains of rhesus macaque MICA and MICB were expressed as a fusion protein with ferritin to generate nanoparticles that displayed both α3 domains on the surface. Nanoparticles formed by this fusion protein were conjugated using click chemistry to CpG ODN 2935 as the adjuvant and characterized by HPLC gel filtration chromatography. Shown are HPLC traces of the protein following conjugation to the CpG oligonucleotide (red: 280 nm trace for detection of protein; blue: 350 nm trace for detection of bis-aryl hydrazone bond). **b**, SDS-PAGE analysis of purified macaque MICA/B α3 – ferritin protein under reducing (+) and non-reducing (–) conditions following CpG conjugation and final purification using a HPLC gel filtration column. **c**–**e**, Characterization of serum antibody responses to rhesus macaque MICA (left) and MICB (right) proteins (full-length extracellular domains without ferritin fusion partner) at different steps in the immunization process. Antibody responses were investigated in three animals (RBQ12, RVf10 and RQq15) at multiple timepoints (pre-immunization; three weeks following initial immunization and boosts 1-3, as illustrated in Fig. 1h) using a fluorescence-based ELISA (RFU, relative fluorescence units) at multiple serum dilutions ($1:10^2$ to $1:10^4$). **f**–**m**, Binding of purified polyclonal serum IgG to cell surface MICA (left) and MICB (right) using HEK293T transfectants that displayed rhesus macaque MICA (Mamu-A*01) or MICB (Mamu-B*01) proteins. Pre-immune sera were used as a control (grey) for sera obtained following immunization (red). Representative histograms (left in **f**, **g**) and graphical summaries of flow cytometry data (right in **f**, **g**, **h**–**m**) are shown for the four immunized macaques (9312, RBQ12, RVf10 and RQq15). Representative data from two experiments (**a**–**b**). Data from a single macaque immunization experiment with technical replicates for each macaque analyzed (**c**–**m**). Two-way ANOVA with Tukey's multiple comparison test (**c**-**e**). Data depict mean+/– SD.

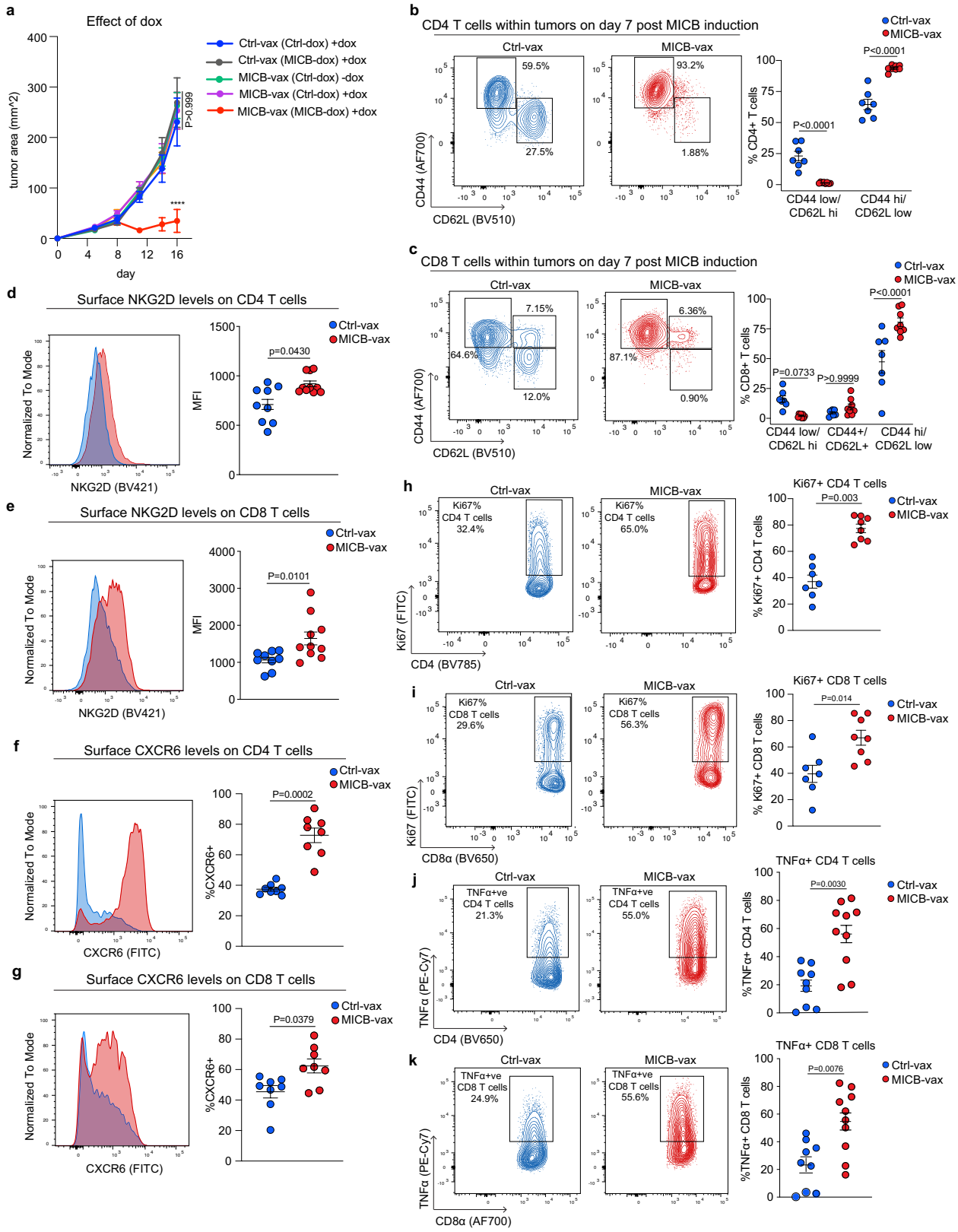

Extended Data Fig. 5 | See next page for caption.

Extended Data Fig. 5 | Impact of vaccine on functional programs of tumor-infiltrating CD4 and CD8 T-cells. a, Effect of doxycycline on tumor growth in vaccinated mice. Mice received Ctrl-vax (blue, grey) or MICB-vax (green, magenta, red) on day 0 and a boost on day 14. B16F10 cells transduced with Ctrl-dox or MICB-dox lentiviral vectors as indicated were implanted on day 21, and mice were treated with doxycycline (or PBS as control) starting on day 25 to induce MICB expression on tumor cells (n=5 mice/group). **b**–**k**, Analysis of tumor-infiltrating T-cell populations. Tumor-infiltrating T-cells were analyzed 7 days following induction of MICB expression by tumor cells (n = 7 mice/group). **b**–**c**, Analysis of CD62L and CD44 expression by tumor-infiltrating CD4 (**b**) and CD8 (**c**) T-cells. **d**–**e**, Representative flow plots (left) and quantification (right) of NKG2D receptor expression by CD4 (**d**) and CD8 (**e**) T-cells. **f**–**g**, Representative flow plots and quantification of CXCR6 receptor expression by CD4 (**f**) and CD8 (**g**) T-cells. **h**–**i**, Quantification of proliferating Ki67+ CD4 (**h**) and CD8 (**i**) T-cells. **j**–**k**, Quantification of TNFα positive CD4 (**j**) and CD8 (**k**) T-cells. Two-way ANOVA with Bonferroni's post hoc test (**a**); two-way ANOVA with Tukey's multiple comparison test (**b**–**c**); two-tailed Mann Whitney test (**d**–**k**). Representative data from two independent experiments (**b**–**i**); representative data from three independent experiments (**j**–**k**). Data depict mean+/− SEM.

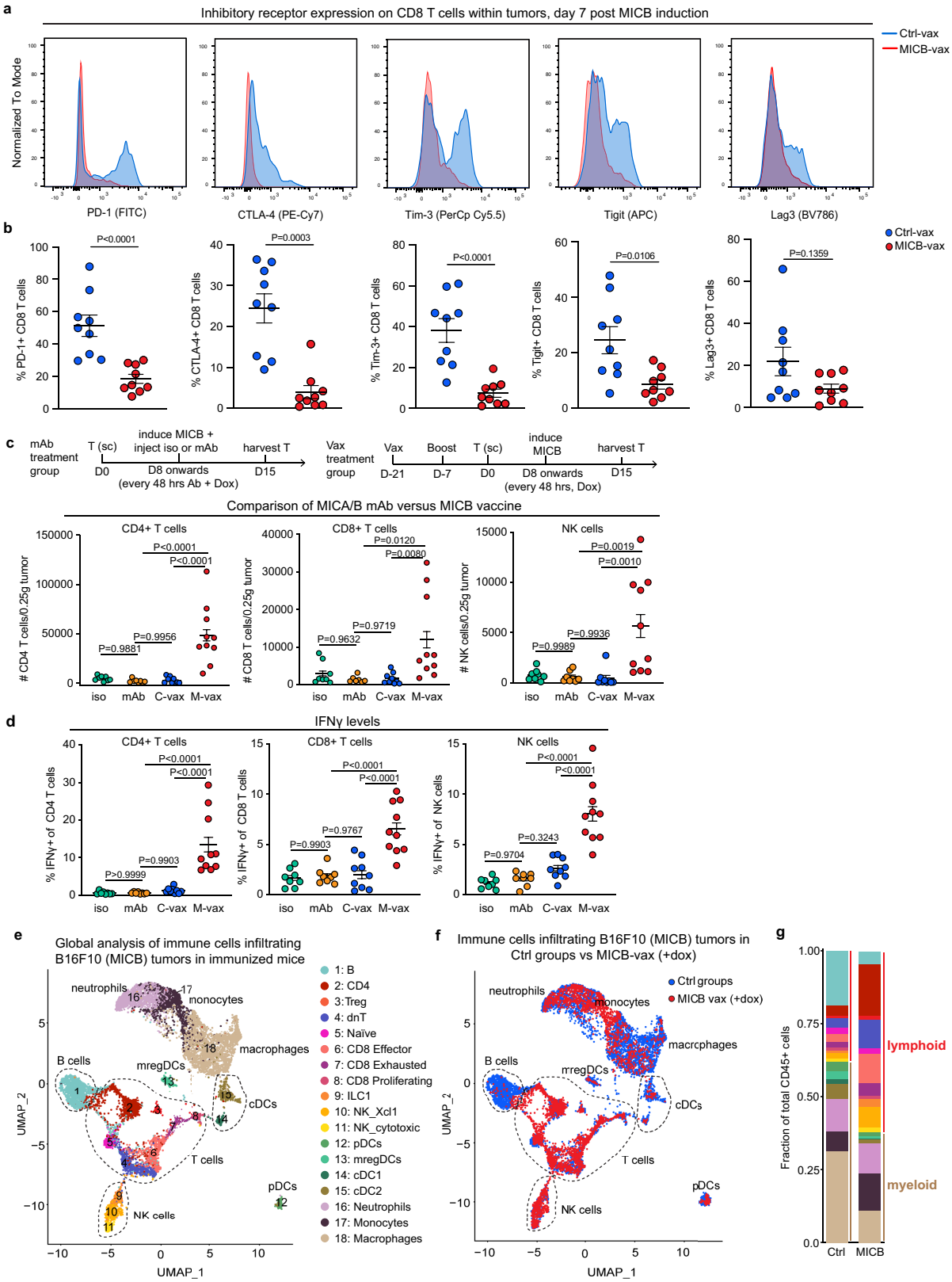

Extended Data Fig. 6 | See next page for caption.

Extended Data Fig. 6 | Flow cytometric and scRNA-seq analysis of changes in tumor-infiltrating immune cells induced by the vaccine.
a–**b**, Representative histograms (**a**) and quantification (**b**) of PD-1, CTLA-4, Tim-3, Tigit and Lag3 expression by tumor-infiltrating CD8 T-cells from Ctrl-vax (blue) or MICB-vax (red) mice (n = 9 mice/group). **c**–**d**, Comparison of T-cell and NK cell populations in B16F10 (MICB) tumors following treatment with a MICA/B mAb or the MICB vaccine. In the vaccine arm, mice received Ctrl-vax (C-vax) (n = 9 mice) or MICB-vax (M-vax) (n = 10 mice) on days 0 and 14, while mice in the mAb treatment group (n = 8 mice/ group) received two buffer injections. Mice were implanted with B16F10 (MICB-dox) tumor cells on day 21. MICB expression was induced on tumor cells by doxycycline treatment starting on day 28, and mice in the mAb treatment group received either mouse IgG2a isotype control mAb (iso) or MICA/B mAb (mAb) treatment every 48 h starting on day 28. Tumor-infiltrating immune cells were analyzed in all groups on day 35. Total numbers of tumor-infiltrating CD4+ T-cells, CD8+ T-cells and NK cells were quantified by flow cytometry (**c**), and intracellular staining was performed for IFNγ (**d**) in all four treatment groups. **e**–**g**, scRNA-seq analysis of changes in tumor-infiltrating immune cells induced by the vaccine. CD45+ immune cells in B16F10 (MICB-dox) tumors were investigated by scRNA-seq under four experimental conditions: the MICB-vax (+dox) experimental group and the three control groups, Ctrl-vax (-dox), Ctrl-vax (+dox) and MICB-vax (-dox). Doxycycline was administered to mice for seven days prior to scRNA-seq analysis to induce MICB expression on tumor cells in two of these groups (+dox). For each of the four groups, CD45+ immune cells were pooled from five mice to reduce variation from individual tumors. **e**, UMAP projection of CD45+ immune cells combined from all experimental groups. Major immune cell populations are annotated based on differentially expressed genes. **f**, Comparison of immune subpopulations across all clusters for the experimental MICB-vax (+dox) group (red) versus the three combined control groups (blue). **g**, Distribution of CD45+ cells across individual clusters (color-coded as in **e**) for the experimental MICB-vax (+dox) group (MICB) and the three combined control groups (Ctrl). Representative data of two experimental repeats (**a**–**b**). Data from a single experiment (**c**–**d**). ScRNA-seq data from a single experiment with sorted CD45+ cells pooled from 5 mice/group (**e**–**g**). Two-tailed Mann Whitney test (**b**); one-way ANOVA with Tukey's multiple comparison test (**c**–**d**). Data depict mean+/− SEM.

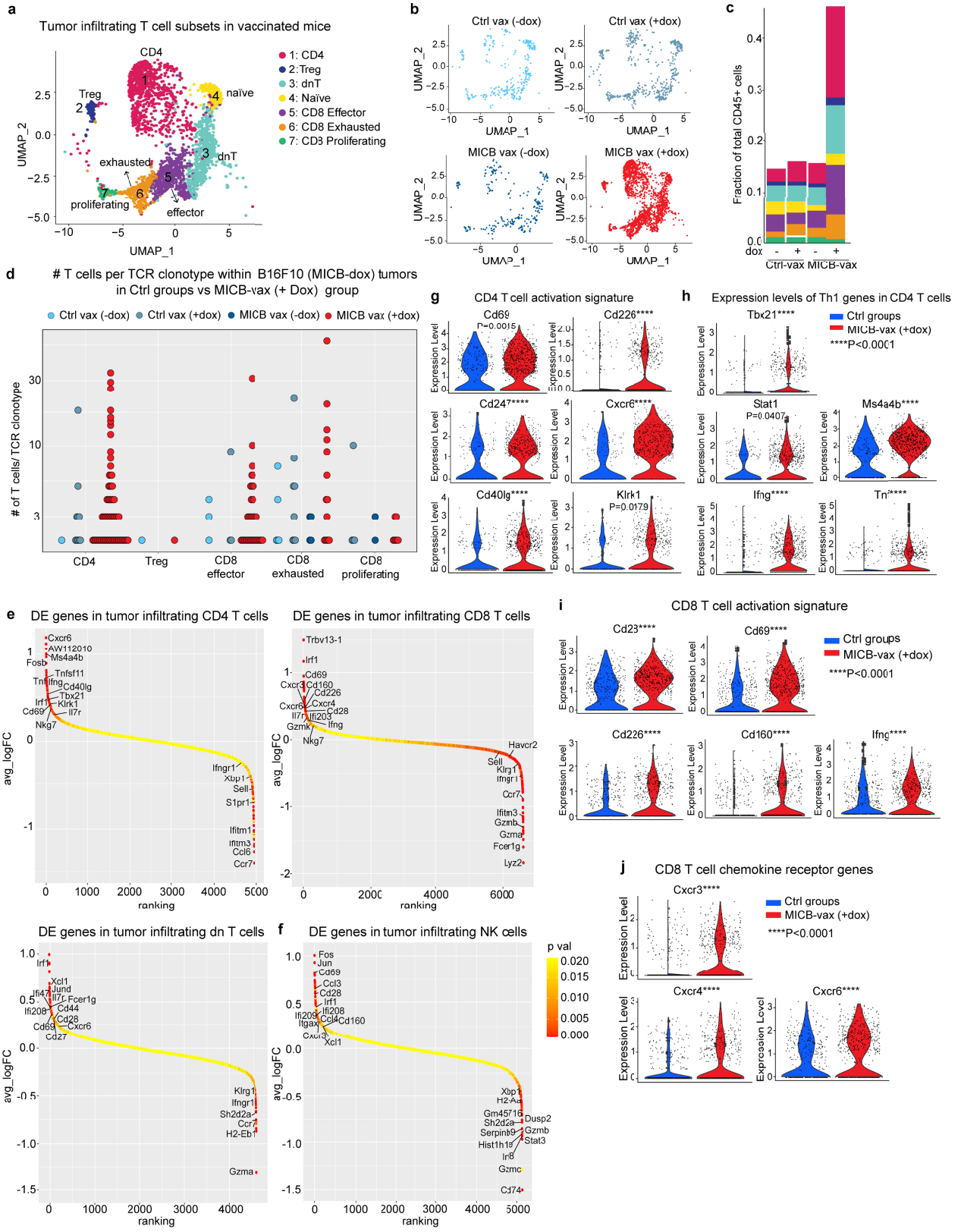

Extended Data Fig. 7 | See next page for caption.

Extended Data Fig. 7 | Gene expression programs of tumor-infiltrating T-cell and NK cell populations. a–**d**, scRNA-seq analysis of T-cell clusters among CD45+ tumor-infiltrating cells in B16F10 (MICB-dox) tumors. UMAP representation of T-cell subclusters (**a**) and visualization of T-cell populations for the experimental MICB-vax (+dox) group (MICB) and the three control groups (**b**). **c**, Contribution of each T-cell subcluster to the total CD45+ immune population for each of the four treatment groups. **d**, Quantification of expanded TCR clonotypes for CD4, Treg, CD8 effector, CD8 exhausted and CD8 proliferating clusters shown for all four treatment groups. **e, f**, Ranking of differentially expressed genes in scRNA-seq data from the indicated T-cell subpopulations (**e**) and NK cells (**f**) comparing cells from the experimental MICB-vax (+dox) group to cells from the three combined control groups, Ctrl-vax (-dox), Ctrl-vax (+dox) and MICB-vax (-dox). **g**–**j**, Violin plots showing expression levels of activation-related genes (**g**) and Th1-related genes (**h**) in CD4 T-cells as well as activation-related genes (**i**) and chemokine receptor genes (**j**) in CD8 T-cells from the experimental MICB-vax (+dox) group compared to cells from the three combined control groups (Ctrl). ScRNA-seq data from a single experiment with sorted CD45+ cells pooled from 5 mice/group (**a**–**j**). Pairwise Wilcoxon rank sum test (**g**–**j**).

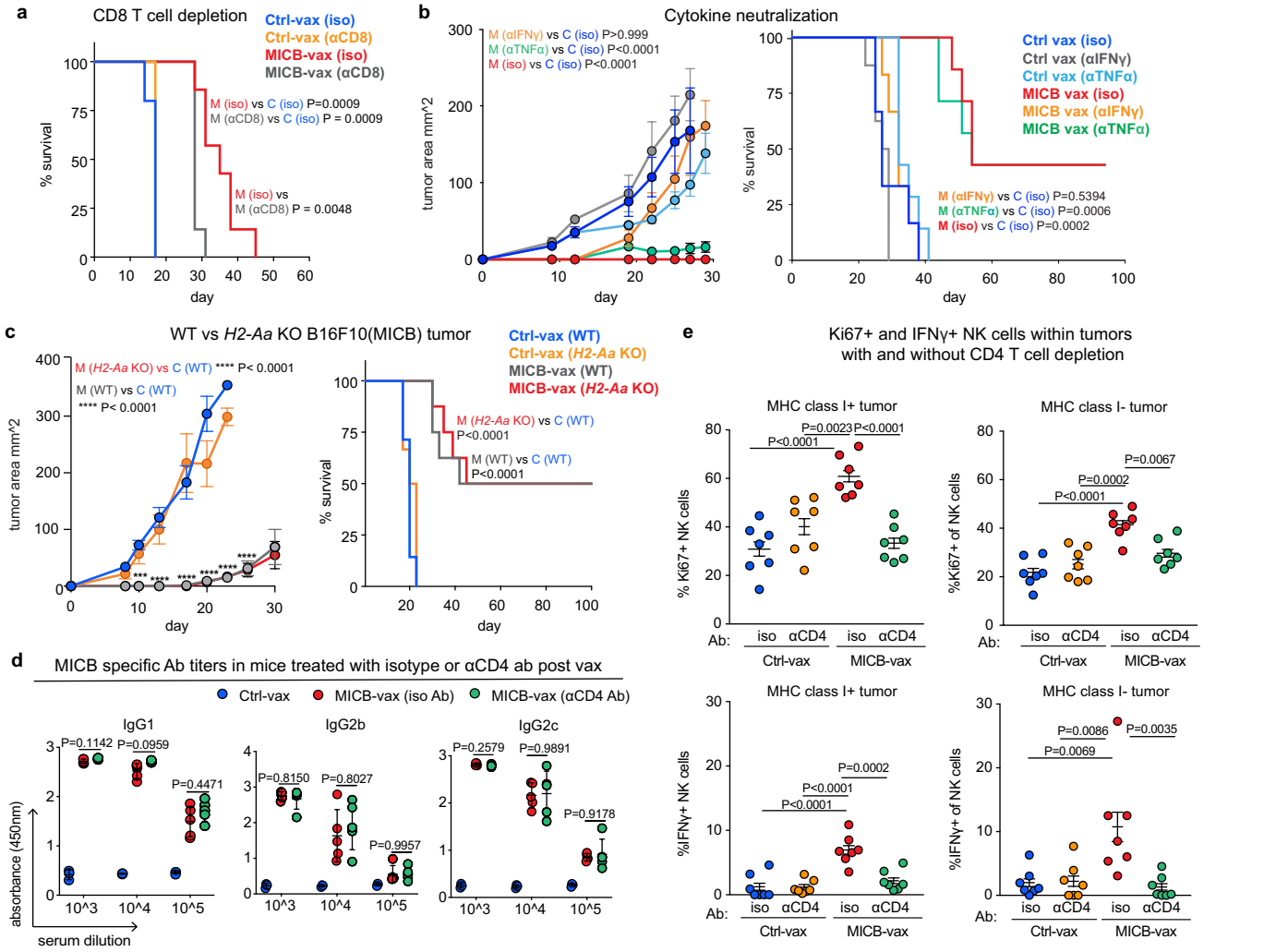

Extended Data Fig. 8 | T cell and NK cell responses in MHC-I expressing and MHC-I deficient tumors. a, Contribution of CD8 T cells to vaccine efficacy. Mice were first immunized with MICB-vax or Ctrl-vax (d0, d14), treated with either isotype control mAb, depleting mAb targeting CD8 T-cells starting on day 21, followed by implantation of B16F10 (MICB) tumor cells (n = 7 mice/ group). **b**, Impact of IFNγ versus TNFα neutralization on the efficacy of the MICB α3 domain vaccine. MICB-transgenic mice received IFNγ or TNFα neutralizing mAbs or an isotype control mAb every 48 h, starting two days prior to subcutaneous injection of B16F10 (MICB) tumor cells on day 21 following immunization (n = 7 mice/group). Tumor growth (left) and survival analysis (right) are shown. **c**, Comparison of vaccine efficacy against B16F10 (MICB) wild-type tumors and tumors with resistance mutation in *H2-Aa* gene. Mice received MICB-vax (n=8 mice/ group) or Ctrl-vax (n = 7 mice/ group) and were then challenged with tumors of the indicated genotypes. **d**, Quantification of MICB-specific serum Ab titers in mice immunized with Ctrl-vax (blue) or MICB-vax followed by treatment with CD4 T-cell depletion (green) or control (red) mAbs for 3 weeks, starting on day 28 following immunization (n=5 mice/group). **e**, Impact of CD4 T-cell depletion on vaccine-induced NK cell infiltration into tumors. Flow cytometric quantification of the percentage of Ki67+ NK cells (top) and IFNγ+ NK cells (bottom) in WT (left) and *B2m*-KO (right) tumors for the following treatment groups: Ctrl-vax + isotype mAb (blue), Ctrl-vax + anti-CD4 (orange), MICB-vax + isotype mAb (red) and MICB-vax + anti-CD4 (green); (n = 7 mice/group). Representative data from two independent experiments (**a-c, e**). Data from a single experiment with technical triplicates (**d**). Log-rank (Mantel-Cox) test (**a**); two-way ANOVA with Bonferroni's post hoc test (**b** left, **c** left) and Log-rank (Mantel-Cox) test (**b** right, **c** right); two-way ANOVA with Tukey's multiple comparison test (**d**); one-way ANOVA with Tukey's multiple comparison test (**e**).

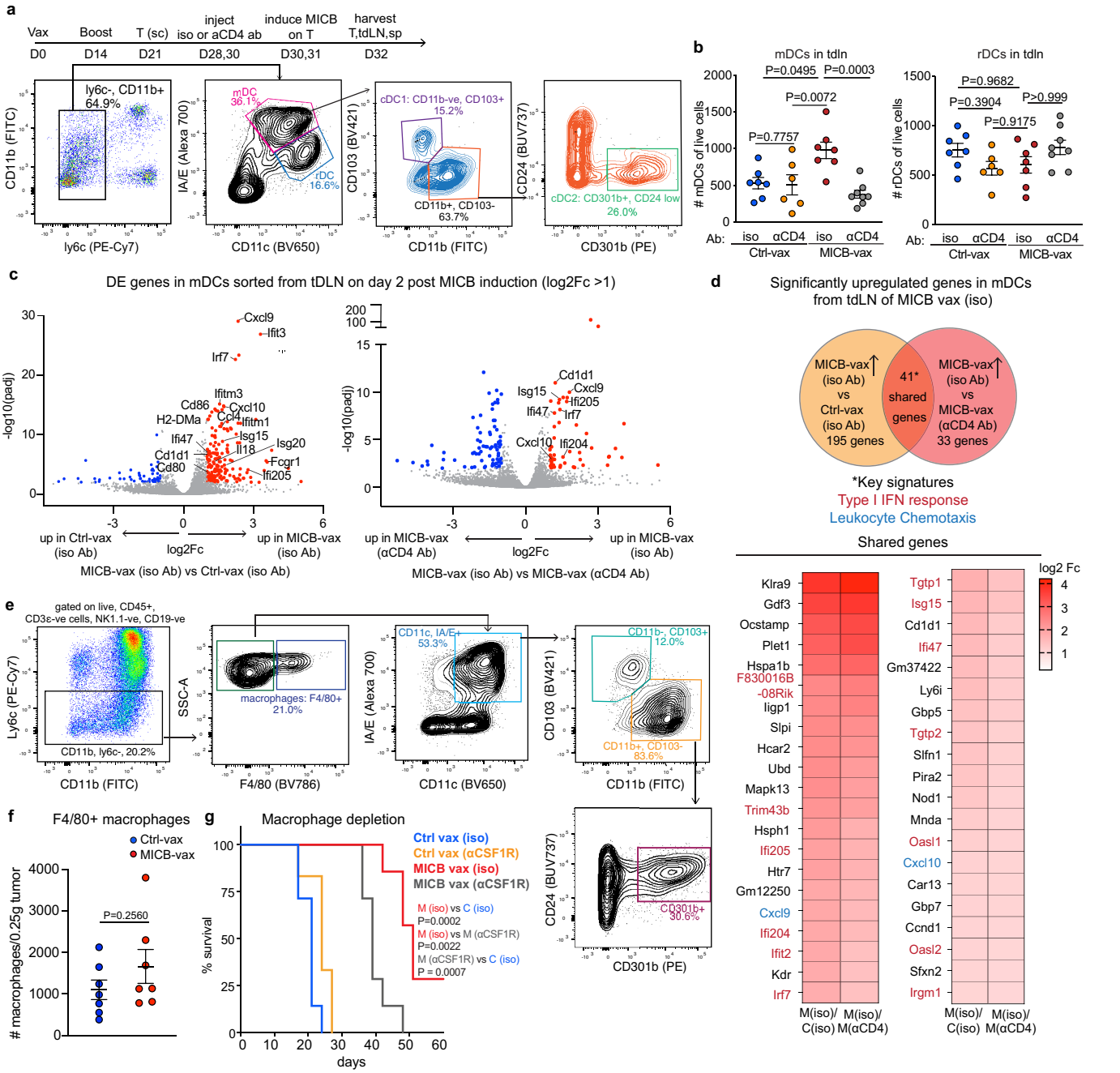

Extended Data Fig. 9 | Characterization of dendritic cells in the tumor draining lymph nodes of vaccinated mice. a, Experimental outline and gating strategy for identification of migratory DC (mDC) subsets within the tumor draining lymph node (tdLN) of immunized mice by flow cytometry. **b**, Impact of CD4 T-cell depletion on mDC and resident (rDC) populations in tdLN of vaccinated mice. DC populations were analyzed in tdLN on day 32, two days following induction of MICB expression on tumor cells with dox (n = 7 mice per group, except in control-αCD4 ab (n = 6 mice). **c**, Differentially expressed genes of mDCs (bulk RNA-seq) sorted from tdLN of MICB-vax and Ctrl-vax mice treated with CD4 depleting (αCD4) or isotype control (iso) mAb. **d**, Upregulated genes in mDCs from the MICB-vax (isotype control mAb, iso) group compared to either MICB-vax plus CD4 T-cell depletion (αCD4) or the Ctrl-vax (isotype mAb) groups. Venn diagram and heatmap of genes with higher expression in MICB-vax (iso) compared to both other groups. **e**–**g**, Characterization of myeloid cells within the tumors of vaccinated mice. Mice were immunized (d0 and 14), B16F10 (MICB-dox) tumor cells were implanted on day 21 and MICB expression was induced on tumor cells on day 28 by doxycycline (dox) treatment. Tumor-infiltrating myeloid cells were analyzed 7 days later. **e**, Gating strategy used for identification of tumor-infiltrating CD103+ cDC1, CD301b+ cDC2 and F4/80+ macrophages in vaccinated mice by flow cytometry. **f**, Quantification of macrophage population within tumors of Ctrl-Vax (blue) and MICB-vax (red) mice on day 7 following MICB induction on tumors with dox (n = 7 mice/group). **g**, Impact of αCSF1R treatment on immunity to B16F10 (MICB) tumors. Mice were immunized with Ctrl-vax or MICB-vax; treatment with αCSF1R or isotype control Ab was started two days prior to subcutaneous injection of B16F10 (MICB) tumor cells; mAb treatment was continued every third day; n=7 mice/group. Data representative of two independent experiments (**a**–**b, e**–**g**). Data from one experiment with three biological replicates per sample. DCs from 3 mice were pooled for each biological replicate (n = 9 mice/group). Significance was determined using thresholds of -log10 >2 (adjusted P value), and log2 >1 (fold change) (**c**–**d**). One-way ANOVA with Tukey's multiple comparison test (**b**); Two-tailed Mann Whitney test (**f**); log-rank (Mantel-Cox) test (**g**). Data represent mean +/− SEM.

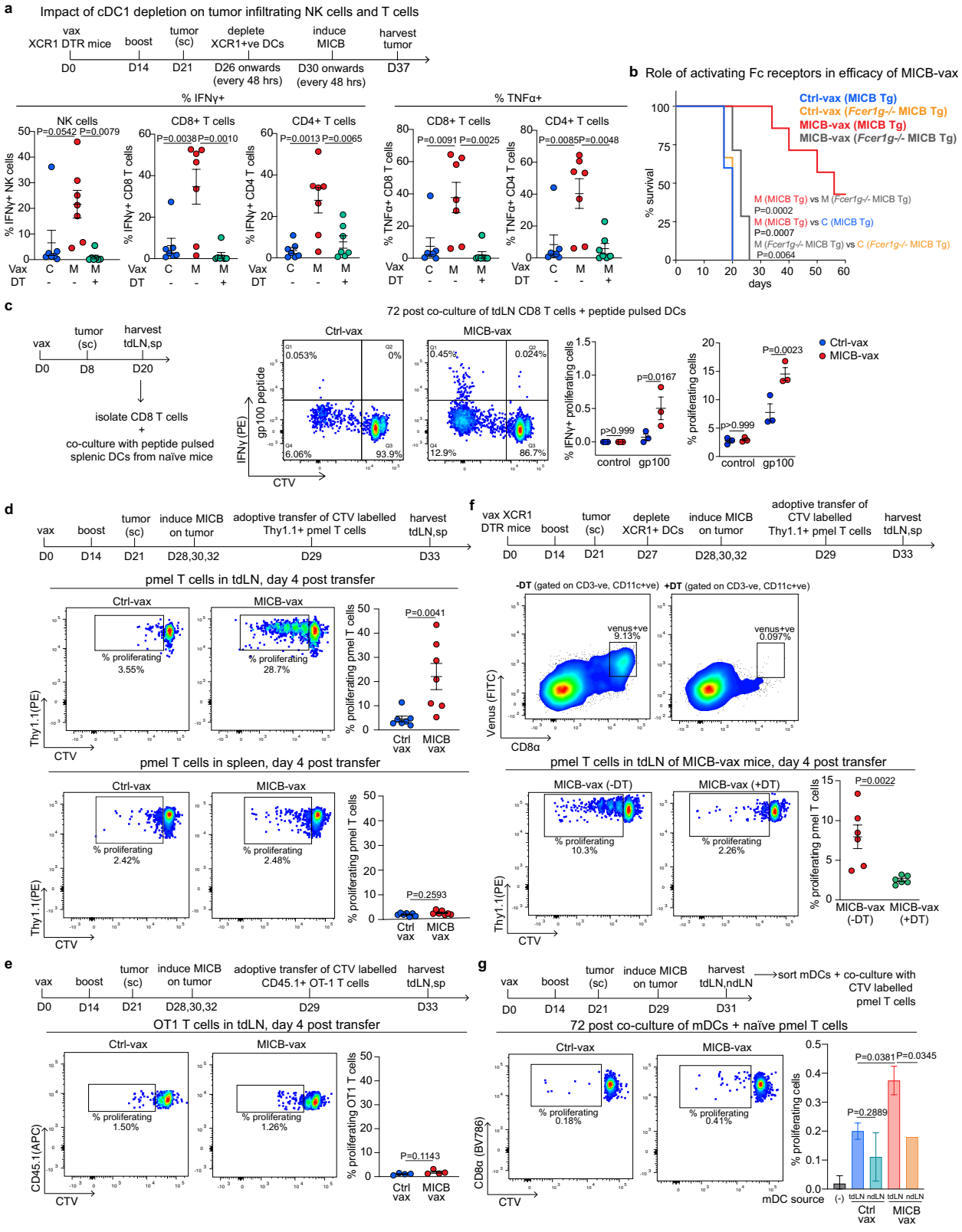

Extended Data Fig. 10 | See next page for caption.

Extended Data Fig. 10 | Cross-presentation of endogenous melanoma antigen by dendritic cells from MICB-vax mice. a, Impact of cDC1 depletion on MICB vaccine-induced T-cell and NK accumulation within tumors in *Xcr1*^{DTR} mice. Mice were treated +/− diphtheria toxin (DT) starting on day 26 following immunization with Ctrl-vax (C) or MICB-vax (M) (days 0 and 14) and B16F10 (MICB-dox) tumor implantation (day 21). Immune cells were analyzed in tumors 7 days following MICB induction on tumors with dox (day 37) (n = 7 mice/group). **b**, Contribution of activating Fc receptors to efficacy of MICB-vax. Survival curves of *FceR1g*$^{-/-}$ MICB-Tg versus MICB-Tg mice immunized with Ctrl-vax (blue) and MICB-vax (red) (n = 7 mice/group). **c**, Analysis of endogenous gp100 specific CD8 T-cell responses. CD8 T-cells were isolated from tdLN of mice immunized with MICB-vax or Ctrl-vax, labeled with the CTV cell proliferation dye and then co-cultured for 72 h with DCs pulsed with control (Ova) or gp100 peptide (10µg/ml). Intracellular cytokine staining (IFNγ) and CTV dilution are shown in representative flow cytometry plots (left); data are quantified for T-cells from both vaccine groups (3 mice/group, right). **d**, Proliferation of transferred CD8 T-cells specific for the gp100 melanoma antigen (from Pmel-1 transgenic mice) in tumor-draining lymph nodes of mice immunized with MICB-vax compared to Ctrl-vax. Mice were vaccinated twice (days 0 and 14) and B16F10 (MICB-dox) tumor cells were implanted subcutaneously on day 21. Doxycycline treatment was initiated on day 28 to induce MICB expression on tumor cells, one day prior to transfer of Thy1.1+ Pmel-1 CD8 T-cells (2x10^6 cells/mouse). Proliferation of CTV-labeled Pmel-1 T-cells was analyzed in tumor-draining LN (top) and spleen (bottom, control organ) four days following T-cell transfer. Cells were gated based on CD3, CD8 and Thy1.1 markers; shown is Thy1.1 marker of transferred Pmel-1 T-cells (Y-axis) and CTV dye dilution in proliferating T-cells (X-axis). Proliferating T-cell populations are indicated in representative flow plots (left) and quantification is shown (right) across the entire cohort of Ctrl-vax (blue) versus MICB-vax (red) mice (n = 7 mice/group). **e**, Control experiment for (**d**) with CD8 T-cells of irrelevant specificity (OT-1 T-cells, n = 4 mice/group). **f**, Role of XCR1+ DCs in the activation of transferred gp100-specific pmel-1 CD8 T-cells. *Xcr1*^{DTR} mice were immunized with MICB-vax (days 0 and 14), and B16F10 (MICB-dox) melanoma cells were implanted on day 21. XCR1+ DCs were depleted by injection of diphtheria toxin (+DT, green) or solvent as a control (-DT, red) one day prior to induction of MICB expression by tumor cells with doxycycline. Thy1.1+ Pmel-1 CD8 T-cells were transferred and proliferation of these T-cells was analyzed in tdLN four days later by dilution of the CTV dye. Top flow cytometry plots show depletion of XCR1+ cells (Venus fluorescent reporter protein) in diphtheria toxin (+DT) treated mice (right) compared to control mice (-DT, left), six days following initiation of DT treatment. Bottom flow cytometry plots show proliferation of transferred pmel-1 CD8 T-cells based on dilution of the CTV dye (X-axis); data are quantified on the right (n=6 mice/group). **g**, Presentation of gp100 peptide by migratory DCs from MICB-vax mice. Naïve Pmel-1 CD8 T-cells were co-cultured for 72 h with migratory DCs (mDC, CD11c+, IA/E high) isolated from tdLN or non-tumor draining LN of Ctrl-vax or MICB-vax mice (pooled from 10 mice/group) implanted with B16F10 (MICB) tumor cells. CD8 T-cell proliferation was assessed based on CTV dilution. Data are representative of two independent experiments (**a-d, f-g**). Data from a single experiment (**e**). One-way ANOVA with Tukey's multiple comparison test (**a**); log rank (Mantel-Cox) test (**b**); two-tailed Mann Whitney test (**c-f**); one-way ANOVA with Dunnett's multiple comparison test (**g**). Data depict mean +/− SEM (**a, c−f**) or mean +/− SD (**g**).